Catalysis Science & Technology

ROYAL SOCIETY OF CHEMISTRY

PAPER

View Article Online
View Journal

Cite this: DOI: 10.1039/d6cy00297h

Activation of isocyanates with gold: towards Au-catalyzed C–H amidation of pyrroles

Francesco Ravera,[abc] Alessandro Bortoli,[a] Juan José Gamboa-Carballo,[d] Sonia Mallet-Ladeira,[e] Karinne Miqueu,[d] Didier Bourissou *[c] and Andrea Biffis *[ab]

Received 9th March 2026,
Accepted 11th May 2026

DOI: 10.1039/d6cy00297h

rsc.li/catalysis

The intermolecular hydroarylation of isocyanates with pyrroles was found to be efficiently catalyzed by the Au(I) complex IPrAuNTf$_2$ (IPr = *N*,*N*′-bis(2,6-diisopropylphenyl)-imidazol-2-ylidene). The transformation tolerates electron-withdrawing and electron-donating substituents both at the heterocycle and the isocyanate. It affords secondary aromatic amides in a single step under mild conditions with catalyst loadings down to 0.5 mol%. The reaction proceeds *via* coordination of the isocyanate to gold and outer-sphere nucleophilic attack of the heterocycle. Several gold(I) isocyanate adducts were authenticated by multinuclear NMR spectroscopy at low temperatures. ^{15}N-labeling of the organic fragment allowed us to observe a deshielding of the ^{13}C NMR N═C═O signal and a decrease of the associated $^{1}J_{CN}$ coupling constant upon coordination to gold. With further support from density functional theory (DFT) calculations, the ground state was assigned to an η^1-*N*-coordination isomer. The corresponding η^1-*O*-adduct lies *ca.* 8–11 kcal mol^{-1} higher in energy. A gold(I) π-adduct involving *N*-methyl pyrrole as the substrate was also authenticated experimentally, including by X-ray crystallography. The latter species is involved as an off-cycle resting state in the catalytic transformation.

Introduction

Gold catalysis has experienced an impressive growth over the past two decades, mainly due to the high affinity of gold cationic complexes for CC π-bonds. The *Umpolung* reactivity of alkynes, alkenes and allenes, stemming from their π-coordination to gold,[1–3] makes these motifs versatile entry points for a broad range of transformations.[4–13] These reactions usually occur under mild conditions and with precise stereo- and regio-selectivity.[14–16] Among these π-systems, alkynes have played a central role in advancing cationic gold catalysis so far.[10,12,15,17,18] Over the past 20 years, significant insight has been gained into the bonding characteristics and reactivity profiles of gold/alkyne π-complexes.[19–26]

Despite significant advances in gold π-acid catalysis, fundamental studies and catalytic transformations involving hetero-unsaturated substrates, *i.e.* CX π-systems (with X = N, O, and S), remain comparatively underexplored.[27–29] A noteworthy example though is the catalytic ring expansion and functionalization of 2*H*-azirines with isocyanates reported by Hashmi and co-workers in 2019 using $AuBr_3$ (Fig. 1A).[30]

In this study, we explored the catalytic hydroarylation of isocyanates. The gold(I) complex (IPr)AuNTf$_2$ was found to efficiently promote the direct C–H amidation of *N*-based heterocycles (namely pyrroles and indoles, Fig. 1B).

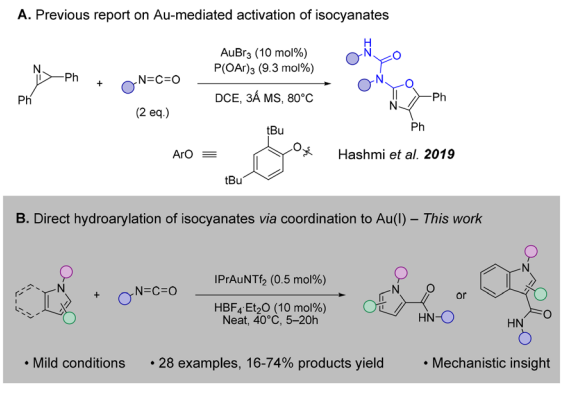

Fig. 1 Gold catalysis with isocyanate substrates.

[a] *Dipartimento di Scienze Chimiche, Università di Padova, via Marzolo 1, Padova 35131, Italy. E-mail: andrea.biffis@unipd.it*
[b] *Consorzio Interuniversitario per le Reattività Chimiche e la Catalisi (CIRCC), Dipartimento di Scienze Chimiche, Università di Padova, via Marzolo 1, Padova 35131, Italy*
[c] *Laboratoire Hétérochimie Fondamentale et Appliquée (LHFA, UMR 5069), CNRS/Université de Toulouse, Toulouse 31062, France. E-mail: didier.bourissou@utoulouse.fr*
[d] *Institut des Sciences Analytiques et de Physico-Chimie pour l'Environnement et les Matériaux (IPREM, UMR 5254), CNRS/Université de Pau et des Pays de l'Adour, Pau 64053, France*
[e] *Institut de Chimie de Toulouse (UAR 2599), Toulouse 31062, France*

Mechanistic investigations suggest an outer-sphere nucleophilic addition pathway involving gold(I)/isocyanate adducts, which were characterized in solution by multinuclear NMR spectroscopy. Surprisingly, although the organometallic chemistry of isocyanates is well established,[31] to our knowledge, no complexes with group 11 metals have been reported so far. A gold(I)/pyrrole π-complex was identified as a resting state of the catalytic cycle, completing the mechanistic picture of this TM-catalyzed hydroarylation of isocyanates *via* electrophilic activation of the NCO moiety.

Results and discussion

Reaction discovery and optimization

The amidation of *N*-methyl pyrrole (**1a**) with phenyl isocyanate (**2a**) was benchmarked as a model reaction (Table 1; complete screening data are collected in Scheme S2).[32] In particular, we probed the reactivity of the system in the presence of (IPr)AuNTf$_2$ as the catalyst, where IPr is the *N*-heterocyclic carbene ligand *N*,*N*′-bis(2,6-diisopropylphenyl) imidazol-2-ylidene, and using the ionic liquid [BMIM][NTf$_2$] as the reaction medium (BMIM = 1-butyl-3-methylimidazolium). We previously disclosed the enhanced efficiency imparted by ionic liquids with respect to ordinary organic solvents, due to the possible stabilization of the cationic intermediates and improved proton shuttling across the different stages of the catalytic cycle.[33–35] The C2-amidation product **3aa** was obtained in 59% yield after 24 h using a 2.5 mol% loading of the gold complex (IPr)AuNTf$_2$ (entry 3). In line with our previous studies, the presence of a sub-stoichiometric amount of an acidic additive, namely HBF$_4$·Et$_2$O (10 mol%), promoted faster reaction kinetics and improved the yield of **3aa** (entry 2, 85% yield).[35,36] On the other hand, the acidic conditions enabled the reaction to proceed with a reduced amount of gold catalyst (0.5–1 mol%), obtaining analogous yields to those achieved under neutral conditions after one day of reaction (entries 1 and 4). The precise role and mode of action of the acid additive is difficult to decipher. For example, it may help in the final stage of the reaction (involving formal proton shuttling) or it may assist gold in the electrophilic activation of the isocyanate. Interestingly, the C3-amidation product **3aa′** was formed in minor amounts (**3aa**:**3aa′** ≈ 10:1). The selectivity ratio between **3aa** and **3aa′** seems to be driven by

Table 1 Reaction optimization[a]

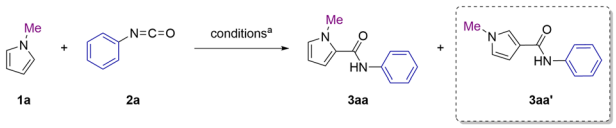

Entry	Catalyst	Solvent	Other variations	Yield **3aa**[b] (%)
1	IPrAuNTf$_2$	[BMIM][NTf$_2$]	—	57
2	IPrAuNTf$_2$	[BMIM][NTf$_2$]	[Au] (2.5 mol%)	85
3	IPrAuNTf$_2$	[BMIM][NTf$_2$]	[Au] (2.5 mol%) no HBF$_4$·Et$_2$O	59
4	IPrAuNTf$_2$	[BMIM][NTf$_2$]	[Au] (1 mol%)	66
5	IPrAuNTf$_2$	[BMIM][NTf$_2$]	2 equiv. **1a**	57
6	IPrAuNTf$_2$	[BMIM][NTf$_2$]	2 equiv. **2a**	71
7	IPrAuNTf$_2$	Acetonitrile	—	9
8	IPrAuNTf$_2$	1,4-Dioxane	—	11
9	IPrAuNTf$_2$	Toluene	—	10
10	IPrAuNTf$_2$	DCM	—	74
11	IPrAuNTf$_2$	Neat	—	65 (3 h) 63[c] (5 h)
12	JohnphosAuCl/AgNTf$_2$	DCM	—	34
13	Ph$_3$PAuCl/AgNTf$_2$	DCM	—	36
14	MeDalphosAuCl/AgNTf$_2$	DCM	—	25
15	(^{t}Pr$_2$P,C)AuI$_2$/2AgNTf$_2$	DCM	—	64
16	IPrAuNTf$_2$	DCM	1 equiv. aniline (0.5 mmol)	0[d] (3 h)
17	—	Neat	—	15 (3 h)
18	—	[BMIM][NTf$_2$]	—	16
19	—	[BMIM][NTf$_2$]	No HBF$_4$·Et$_2$O employed	0

[a] [Au] (0.5 mol%), HBF$_4$·Et$_2$O (10 mol%), [**1a**] = [**2a**] = 0.67 M, 0.5 mmol scale, 40 °C, 24 h. [b] Yields determined by ^{1}H NMR spectroscopy with dimethyl sulfone as the internal standard (reaction time in parenthesis if different from 24 h). [c] Isolated yield. [d] Complete consumption of phenyl isocyanate with the formation of *N*,*N*′-diphenylurea was detected.

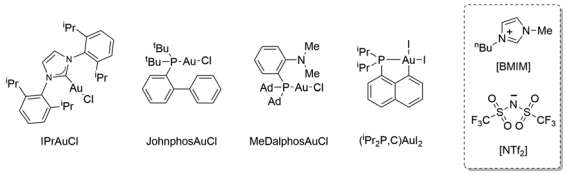

the nucleophilic character of positions 2 and 3 of heterocycle **1a**, with no noticeable differences noticed upon changing the gold pre-catalyst, the reaction temperature, the solvent or the presence or absence of HBF_4. Increasing the temperature from 40 to 60 °C had detrimental effects on the catalytic performance, suggesting low stability of the active species at higher temperatures (38% yield after 24 h at 60 °C, Scheme S2f).[32] Control tests underscored the essential role of the gold complex in promoting reactivity (entries 17–19). In addition, an enhanced reaction rate and a higher yield of **3aa** were recorded in the presence of an excess of isocyanate (71% yield, entry 6), while increasing the amount of nucleophile **1a** did not have any influence on the yield (entry 5). The same trend was observed employing the (^{i}Pr$_2$P,C)AuI$_2$ pre-catalyst (Scheme S2b).[32] Notably, only the complexes IPrAuNTf$_2$ and (^{i}Pr$_2$P,C)Au(NTf$_2$)$_2$ exhibited appreciable catalytic activity among those tested (Scheme S2c).[32] In terms of solvent, [BMIM][NTf$_2$] provides faster initial kinetics, most probably as an effect of the stabilization of cationic species and favorable proton exchange in solution, while a decrease in rate is observed over time. On the other hand, DCM mediates slower kinetics but provides overall higher yields after a 24 h reaction time (entry 10).

This difference is likely due to water traces in the ionic liquid, which may promote the formation of aniline *via* hydration/decarboxylation of the isocyanate.[37] A control test in the presence of aniline confirmed that the production of this by-product influences the reaction efficiency, by consuming isocyanate **2a** (entry 16). All other coordinating solvents resulted in sluggish reactivity with only traces of **3aa** present after 24 h of reaction (entries 7–9). Interestingly, changing the counteranion of the gold complex to hexafluoroantimonate and the reaction solvent to DCM did not enhance catalytic performance (76% yield after 24 h, Scheme S2g),[32] which contrasts with most gold(I)-catalyzed processes, where anion identity usually plays a decisive role.[38–40] Potential contribution of the silver salt (*i.e.* direct activation of **2a** by Ag^+ ions)[41] can be excluded since activation of the complex IPrAuCl with a stoichiometric amount of $AgSbF_6$ produced analogous results to the preformed complex IPrAuNTf$_2$ (Scheme S2f).[32] Ultimately, employing neat conditions proved most effective, increasing the reaction rate and achieving full conversion of **1a** within 3 h (entry 11). Attempts to further increase the yield were unsuccessful: neutral conditions led to lower yields and longer reaction times (46% isolated **3aa** in 20 h), while syringe pump methods provided similar results to bulk conditions (Scheme S2h).[32]

Substrate scope

The generality of this gold-catalyzed direct C–H amidation reaction was then investigated under the optimized conditions (entry 11) on a 0.5–1 mmol scale (Fig. 2). Aryl isocyanates with both electron–withdrawing (EW) and electron–donating (ED) substituents were successfully utilized showcasing a low influence of the electronic effects on the reaction yield. On the other hand, the presence of sterically demanding groups near the nitrogen atom negatively affected the performance (*cf.* the *ortho*, *meta* and *para* methyl-substituted substrates **2i**, **2f** and **2b**). Specifically, mesityl and 2,6–dimethylphenyl derivatives afforded only modest yields after 20 h, whereas the Dipp–substituted isocyanate remained unreactive. This behavior contrasts with methodologies that rely on H-bond catalysis, which are less affected by the *ortho*-substituents on aryl isocyanates, as

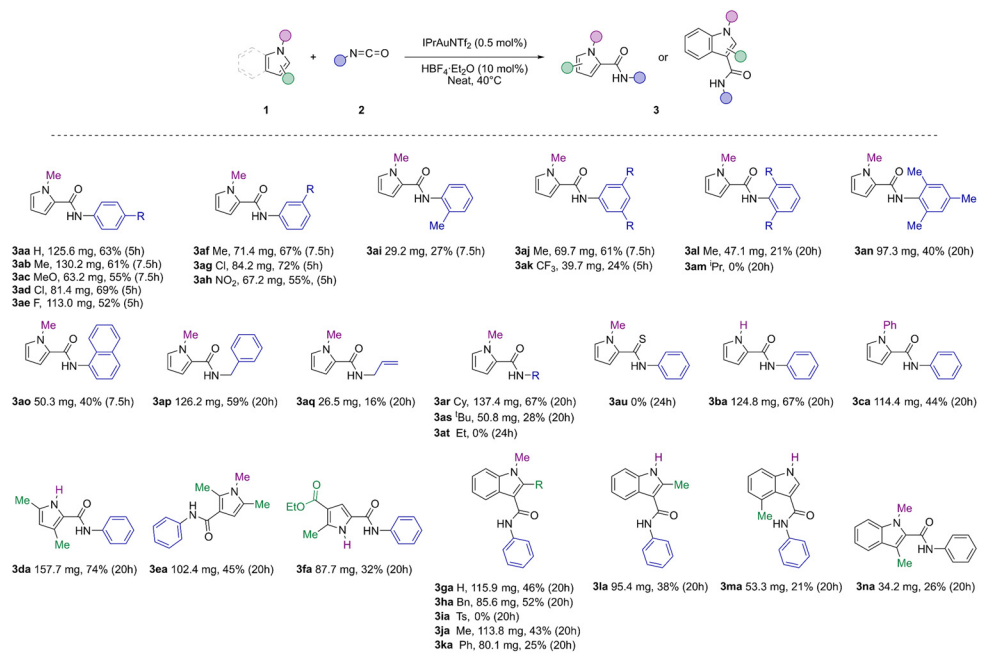

Fig. 2 Reaction scope; isolated yields after column chromatography are reported (reaction time in parenthesis).

independently reported by the groups of Neri and Song.[42,43] The active species in gold catalysis is most likely quite different from the H-bonded aggregates formed in protic environments such as in resorcinarene capsules or HFIP (hexafluoroisopropanol). Other isocyanates bearing unsaturated residues such as naphthyl, benzyl and allyl groups were successfully employed (**2o**, **2p** and **2q**), though with a modest yield for the latter. Ethyl isocyanate and phenyl isothiocyanate failed under the same conditions over a 24 h reaction time (**2t** and **2u**). While the thio-derivative was expected to have a more inert character toward nucleophilic attacks[44] the reason why ethyl isocyanate (**2t**) was found unreactive remains unclear. Conversely, isocyanates substituted by secondary and tertiary alkyl groups were successfully included in the scope, affording the corresponding amidation products **3ar** and **3as** in 67 and 28% yields, respectively. It is worth noting here that methodologies that rely on H-bond catalysis appear instead limited to aryl isocyanates as substrates.[42,43]

The transformation was found to also display good generality with respect to the nucleophile. Both unsubstituted and *N*–phenyl pyrroles showed appreciable reactivity, with a higher yield obtained for the less hindered nucleophile (67% of **3ba** *vs.* 44% of **3ca**). Expectedly, increasing the number of EDGs at the heterocycle enhanced the yield (**3da**, 74% yield). Selective C3-amidation was achieved when the positions nearer to nitrogen were blocked by methyl groups (**3ea**, 45% yield). The introduction of a carboxylate function as an EWG was also possible, albeit increasing the reaction time (**3fa**, 32% yield). Indoles were also shown to be competent substrates, requiring slightly longer reaction times though (20 h typically). *N*-methyl- and *N*-benzyl-indoles were employed first, delivering the corresponding C3-functionalized amides in 46% (**3ga**) and 52% (**3ha**) yields, respectively. Installation of a more electron-deficient substituent at *N* completely suppressed reactivity (*N*-tosyl indole **1i**). Substitution of the C2 position of *N*-methyl indole by a methyl group has little impact (**3ga** and **3ja** are obtained in 43–46% yields). The *N*-unprotected 2-methylindole gave both C3- and N-amidated products in a 1.2 : 1 ratio (determined by ^{1}H NMR), still affording **3la** in 38% yield. With indoles substituted by a phenyl group at C2 or a methyl group at C4, the amidation products **3ka** and **3ma** were obtained in modest yields (25% and 21%, respectively). Moreover, locking both the *N*- and C3-positions enables selective C2 amidation (as for the pyrrole **1e**), and **3na** was obtained in 26% yield. First attempts with other electron-rich (hetero)arenes (*e.g.* mesitylene, 1,3,5-trimethoxybenzene, furan, and 2,3-dimethylfuran) did not give the corresponding amidation products.

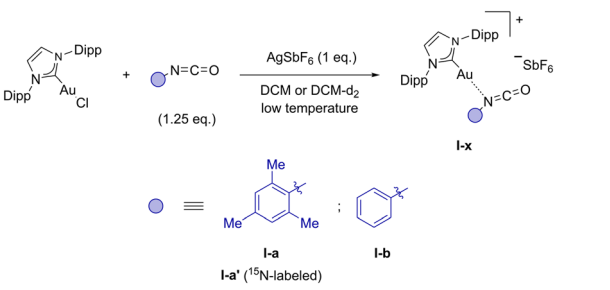

Scheme 1 Reaction of IPrAuCl with isocyanates in the presence of $AgSbF_6$ as an activator.

Characterization of gold(I) isocyanate and pyrrole adducts

With the aim to generate and characterize Au(I) isocyanate adducts, the $IPrAuSbF_6$ complex was generated in the presence of different isocyanates (Scheme 1). The mesityl-substituted derivative (**2n**) was first selected to protect the reactive NCO moiety by steric shielding and the reaction mixture was analyzed by FT-IR spectroscopy in solution.

Unfortunately, the collected data were inconclusive, with only a negligible shift of the antisymmetric N=C=O stretch in the presence of the gold complex $IPrAuSbF_6$. React-IR measurements were also conducted both at −30 °C and room temperature but no clear evidence to support coordination was obtained. Fortunately, NMR spectroscopy proved much more informative. The ^{1}H NMR spectrum of the reaction mixture between $IPrAuSbF_6$ and MesNCO displayed two sets of signals for the isocyanate. One set of signals aligns with those of **2n**, but with a broader peak width. The other one is slightly shielded upfield (by 0.19, 0.29 and 0.26 ppm for the $^{ortho}CH_3$, $^{para}CH_3$ and CH signals, respectively) and the integrations relative to the IPr signals match those expected for a 1 : 1 adduct. ^{13}C NMR spectroscopy showed consistent data. Most signals are slightly deshielded with respect to the free **2n**, except for the *meta* carbon atoms at the mesityl ring,

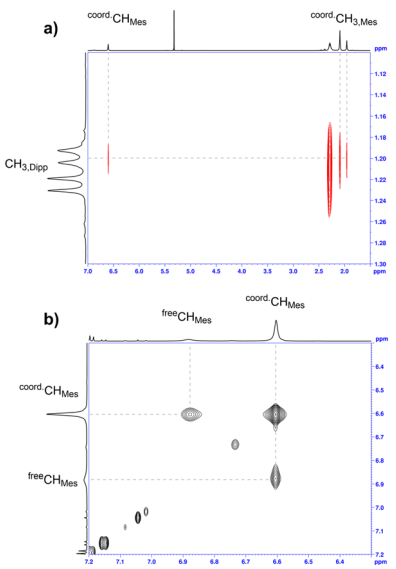

Fig. 3 a) NOESY (600 MHz, DCM-d_2) spectrum; zoom on the NOE cross-peaks between the isocyanate and IPr ligands; b) NOESY (600 MHz, DCM-d_2) spectrum; ligand exchange at **I-a**. Red and black cross-peaks correspond to the negative and positive phases of the signal. A mixing time of 0.7 s was used for the acquisition.

whose signal is shifted downfield by 12.6 ppm. No direct identification of the N═C═O carbon atom was possible at this stage. Nonetheless, coordination of the isocyanate to the $IPrAu^+$ fragment was confirmed by NOESY NMR, showing cross-peaks between the Mes and IPr signals (Fig. 3a), and exchange between free and coordinated **2n** (Fig. 3b).

DOSY analysis also supported coordination.[32] The *D* value calculated from the signals of the coordinated MesNCO ($1.17 \pm 0.02 \times 10^{-9}$ m^2 s^{-1}) matches well with that found for the $IPrAu^+$ fragment ($9.8 \pm 0.3 \times 10^{-10}$ m^2 s^{-1}) and is significantly lower than the *D* value measured for isocyanate **2n** in the absence of the gold complex ($2.20 \pm 0.11 \times 10^{-9}$ m^2 s^{-1}).

^{15}N-labeling of the isocyanate[32] facilitated the identification of the ^{15}N NMR signal for the NCO moiety, with only slight deshielding being observed upon coordination to gold ($\Delta\delta_{15N}$ = 1.7 ppm at −20 °C, Fig. 4a). In addition, a ^{13}C-^{15}N HMBC experiment allowed unequivocal identification of the heteroallene carbon signal, which again shows minimal deshielding with respect to the free isocyanate **2n′** ($\Delta\delta_{13C}$ = 0.9 ppm, Fig. 4b). However, the $^1J_{CN}$ coupling constant was found to significantly decrease upon coordination, from 63.4 Hz in free **2n′** to 50.9 Hz in complex **I-a′**, suggesting some weakening of the C═N bond.

When phenyl isocyanate (**2a**) was used as the substrate for coordination to $IPrAuSbF_6$, only partial formation of the corresponding adduct **I-b** was observed (Scheme 1). Interestingly though, subsequent addition of *N*-methyl pyrrole (**1a**, 1 equiv.) led to the displacement of **2a** and the formation of a new Au(I) complex **II-a** (Scheme 2). Treating the mesityl-substituted isocyanate adduct **I-a** with *N*-methyl pyrrole led to similar observations.

Complex **II-a** could be independently synthesized by coordination of *N*-methyl pyrrole to *in situ* generated

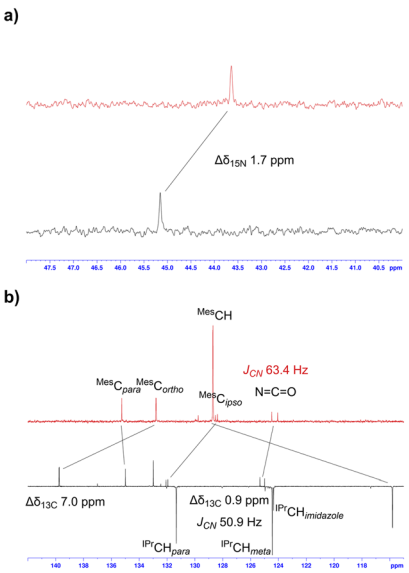

Fig. 4 Stacked ^{15}N NMR spectra (a) and $^{13}C\{^1H\}$ spectra (b) of the ^{15}N-labeled Au(I) isocyanate complex **I-a′** (600 MHz, −20 °C, black line) and free isocyanate **2n′** (500 MHz, −20 °C, red line).

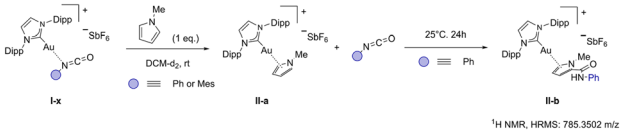

Scheme 2 Displacement of the phenyl isocyanate by *N*-methyl pyrrole at Au(I) and subsequent formation of the amidation product **3aa**.

$IPrAuSbF_6$. Its structure was ascertained by multinuclear NMR spectroscopy and single-crystal XRD analysis (Fig. 5). Guinchard and co-workers have recently described somewhat related cationic Au(I) complexes bearing Buchwald-type phosphines as ancillary ligands and indoles as π-donor moieties.[45] Complex **II-a** exhibits dissymmetric η^2-coordination involving the C2═C3 double bond of *N*-methyl pyrrole with Au–C2 and Au–C3 bond lengths of 2.212(10) and 2.532(11) Å, respectively. These Au–C bond lengths fall in the typical range of those found previously in π-arene and alkene Au(I) complexes bearing phosphines and NHCs.[46–48] The C2═C3 bond is slightly lengthened upon coordination compared to the C4═C5 bond, with bond lengths of 1.402(17) and 1.321(16) Å, respectively.

NMR spectroscopy further confirmed the π-coordination of *N*-methyl pyrrole and disclosed some dynamic behavior in solution. The ^1H and ^{13}C NMR spectra of **II-a** display only 2 sets of signals for the pyrrole ring, as for the free *N*-heterocycle, indicating chemical equivalence of the C_2–H/C_5–H and C_3–H/C_4–H moieties at the NMR timescale. It is likely that the $IPrAu^+$ fragment easily shifts over the pyrrole π-system with the η^2-coordinated complex as the ground-state structure. Nonetheless, the ^1H NMR signals of *N*-methyl pyrrole shift significantly upon coordination, to highfield for the $H_{2/5}$ and H_{Me} atoms (by 0.16 and 0.25 ppm, respectively) and to downfield for the $H_{3/4}$ atoms (by 0.27 ppm). ^{13}C NMR spectroscopy also shows noticeable differences between complex **II-a** and free *N*-methyl pyrrole, in particular for the signals of the aromatic ring. The C_2/C_5 signal shifts downfield by 7.1 ppm, while the C_3/C_4 signal is found upfield by 10.2 ppm. Complex **II-a** is stable in solution, with only marginal decomposition observed within 1 day at

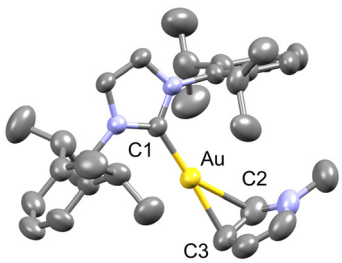

Fig. 5 Molecular structure of complex **II-a**. Hydrogen atom, counter-anion and solvent molecules omitted for the sake of clarity. Ellipsoids are represented at 50% probability. Selected bond distances (in Å) and bond angles (in °): Au–C(1) 1.989(7), Au–C(3) 2.212(10), Au–C(2) 2.532(11), C(2)–C(3)–Au 85.8(7), and C(3)–C(2)–Au 60.6(6).

room temperature, even in the presence of air and/or water. Nevertheless, exposing this last species to phenyl isocyanate led to the formation of the product of the C3-amidated pyrrole **3aa** identified by NMR spectroscopy and HRMS as its π-complex **II-b** (Scheme 2). Pyrroles **1a** and **3aa** help to stabilize $IPrAu^+$ under catalytic conditions, *albeit* competing with the isocyanate for coordination at the metal center. In the absence of **1a**, the Au(I) isocyanate adduct undergoes

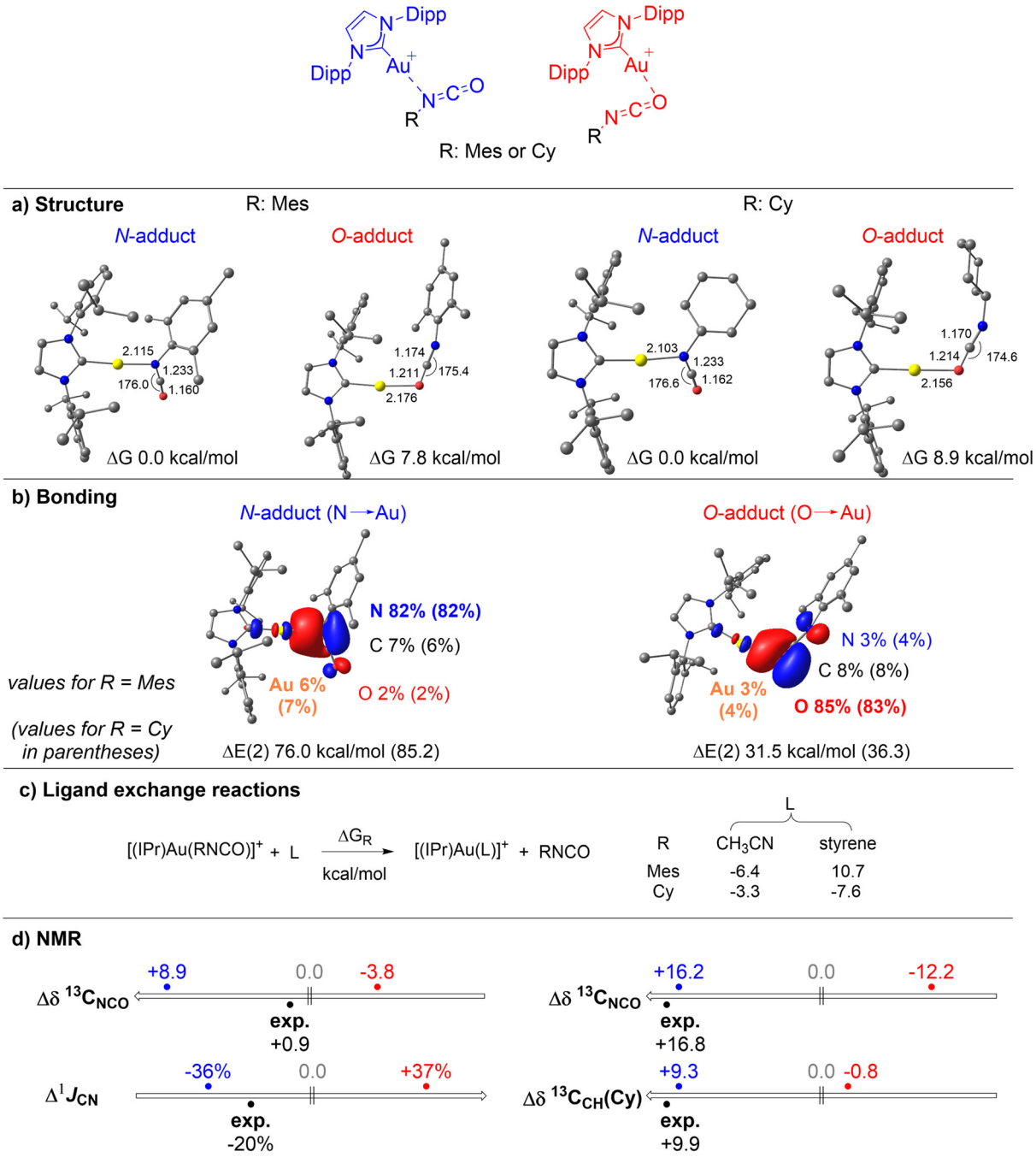

Fig. 6 a) Geometrical data (bond lengths in Å and bond angles in °) and relative free energies (ΔG in kcal mol^{-1}) of the end-on $[(IPr)Au(RNCO)]^+$ complexes (R: Mes and Cy), considering the *N*- and *O*-adducts. Optimizations carried out at the SMD(DCM)-PBE0-D3(BJ)/SDD+f (Au), 6-31G** (other atoms) level of theory. b) Bonding situation from NBO analysis. Plots of the natural localized molecular orbitals (NLMO) (cutoff: 0.03 a.u.) and the contribution of each atom in percent (%). Second-order perturbation stabilizing energies $\Delta E(2)$ in kcal mol^{-1} for N → Au and O → Au donations. c) Gibbs free energy (ΔG_R, in kcal mol^{-1}) for the ligand exchange reactions of the isocyanate Au(I) complexes $[(IPr)AuN(R)CO]^+$ (R: Mes and Cy) with acetonitrile (MeCN) and styrene. d) NMR data computed at the GIAO-SMD(DCM)-PBE0-D3(BJ)/SDD+f(Au), IGLO-II (other atoms)//SMD(DCM)-PBE0-D3(BJ)/SDD+f (Au), 6-31G** (other atoms) level of theory. ^{13}C chemical shift of the NCO group relative to the free ligand ($\Delta\delta_{^{13}C(NCO)}$ in ppm) for the $[(IPr)Au(RNCO)]^+$ complexes (R: Mes and Cy). ^{13}C chemical shift of the CH_{Cy} signal, relative to the free ligand ($\Delta\delta_{^{13}C(Cy)}$ in ppm) for the $[(IPr)Au(CyNCO)]^+$ complex. Change in $^1J_{CN}$(NCO) between the free ligand and the *N*-adducts in% (Δ^1J_{CN}).

decomposition *via* formation of $[(IPr)_2Au][SbF_6]$ or rapid hydration and decarboxylation of the generated carbamate.[49] ^{1}H NMR spectroscopy shows a broad singlet at *ca.* δ 5.2 ppm, diagnostic of the Au(I) aniline complexes $IPrAu(NH_2Ar)^+$, which could be isolated and characterized by multinuclear NMR spectroscopy and HMRS for the mesityl and phenyl isocyanates.[32] The high sensitivity of the Au(I) isocyanate complexes to moisture stands as an experimental evidence of the enhanced electrophilicity of the N═C═O moiety once coordinated to gold.

The coordination of alkyl-substituted isocyanates to gold was also investigated. Multinuclear NMR techniques at low temperatures allowed the coordination of cyclohexyl (**2r**) and benzyl (**2p**) isocyanates at the $IPrAu^+$ fragment to be established (namely complexes **I-c** and **I-d**), while electrophilic activation of the NCO moiety was apparent from ^{13}C NMR spectroscopy (Scheme S29).[32]

Computational studies

To support our experimental findings, density functional theory (DFT) calculations were performed on key Au(I) complexes, *i.e.* the isocyanate complexes $[(IPr)Au(RNCO)]^+$ (R: phenyl, mesityl, and cyclohexyl) and the pyrrole complex $[(IPr)Au(MeNC_4H_4)]^+$ at the SMD(DCM)-PBE0-D3(BJ)/SDD+f(Au), 6-31G** (for all other atoms) level of theory. This study addressed several objectives: (i) to explore the possible modes of coordination for the Au(I) isocyanate complexes and compare the obtained structures and their relative energies, (ii) to analyze the bonding interactions between the isocyanate and the gold complex, (iii) to estimate the binding strength of the isocyanates relative to other labile ligands (*i.e.* acetonitrile and styrene), (iv) to evaluate the influence of the coordination mode (O *vs.* N) on spectroscopic properties (NMR) to draw parallels with the experimental observations and confirm the assigned structures, (v) to analyze the structure and bonding of the *N*-methyl pyrrole Au(I) complex in terms of π-coordination and fluxionality, and (vi) to assess the relative stability of the isocyanate and *N*-methyl pyrrole adducts proposed as reactive species and off-cycle resting state, respectively. The conclusions of these investigations are as follows:

(i) Only end-on complexes were identified on the potential energy surface (PES) for the Au(I) isocyanate adducts, and no side-on structures were located as energy minima (Fig. 6a). The *N*-adduct turned out to be more stable than the *O*-adduct by 7.8 to 11.1 kcal mol^{-1} depending on the R substituent (R = Mes, Ph, and Cy).

(ii) Natural bond orbital (NBO) analysis and energy decomposition analysis (EDA) using the extended transition state-natural orbitals for chemical valence (ETS-NOCV) point out significant donor–acceptor interactions for both coordination isomers. The N → Au interaction in the *N*-adducts is stronger than the O → Au interaction in the *O*-adducts, as is apparent from the contribution of Au in the corresponding natural localized molecular orbitals (NLMOs), the stabilization energies $\Delta E(2)$ obtained by second-order perturbation theory, and the orbital interaction energies $\Delta E(\rho_i)$ obtained by EDA-ETS-NOCV (Fig. 6b).

(iii) The binding strength of the isocyanate in the thermodynamically favored *N*-adduct form was evaluated through displacement reactions, with acetonitrile and styrene as competing ligands (Fig. 6c). From the obtained Gibbs free energy changes (ΔG_R), the isocyanates were found to be only slightly less strongly bound to Au(I) than acetonitrile and styrene, all the more so for CyNCO than MesNCO.

These results are consistent with the fact that Au(I) isocyanate complexes could be spectroscopically characterized at low temperatures.

(iv) Comparing the NMR data computed for the *N*- and *O*-adducts with those of the free isocyanate revealed significant differences, enabling confident structural assignment (Fig. 6d). For the mesityl-substituted isocyanate, *N*-coordination to Au(I) was indeed found to induce deshielding of the ^{13}C NCO signal and a decrease of the $^1J_{CN}$ coupling constant, in line with experimental observations, whereas the corresponding *O*-bound adduct exhibits opposite trends. In the case of CyNCO, the experimentally observed shift of the heteroallene carbon ($\Delta\delta_{^{13}C}$ + 16.8 ppm) closely matches the value calculated for the *N*-adduct (+16.2 ppm) but largely deviates from that corresponding to the *O*-adduct (−12.2 ppm). Additionally, the ^{13}C NMR signal for the CH_{Cy} carbon adjacent to the heteroallene group proved highly diagnostic. Upon coordination of the isocyanate to Au(I), it shifts downfield by +9.3 ppm for the *N*-adduct, in excellent agreement with the shift determined experimentally (+9.9 ppm), while the *O*-adduct shows a slight upfield shift (−0.8 ppm).

(v) For the coordination of *N*-methyl pyrrole to Au(I), a π-complex was located on the PES. It adopts dissymmetric η^2-coordination involving the C═C bond adjacent to the nitrogen atom, with Au–C bond lengths of 2.227 and 2.460 Å (Fig. 7a). The optimized geometry closely matches that determined by single-crystal X-ray diffraction. The dissymmetric nature of the π-coordination is further supported by the NLMO associated with the $\pi_{C=C}$ orbital (Fig. 7b), which shows unequal contributions from the two carbon atoms (36 and 49%). Bonding analysis indicates strong σ-donation from the C═C double bond into the $\sigma^*_{Au(NHC)}$ orbital ($\Delta E(2)$ 79.8 kcal mol^{-1}), accompanied by weak back-donation from the d(Au) orbital into the $\pi^*_{C=C}$ orbital [$\Delta E(2)$ 18.0 kcal mol^{-1}]. In addition, a low-lying transition state involving π-coordination of the C3═C4 bond to Au(I) ($\Delta G^{\neq}$ 2.1 kcal mol^{-1}) was found on the PES, substantiating the facile shift of the Au(I) fragment over the π-system, consistent with NMR observations (Fig. 7a).

(vi) Finally, to support the role of the Au(I) pyrrole π-complex as the catalytic resting state, we examined the displacement of isocyanates for *N*-methyl pyrrole at Au(I) and found these ligand exchanges to be indeed thermodynamically favored by 5.7 to 8.8 kcal mol^{-1} (Fig. 7c).

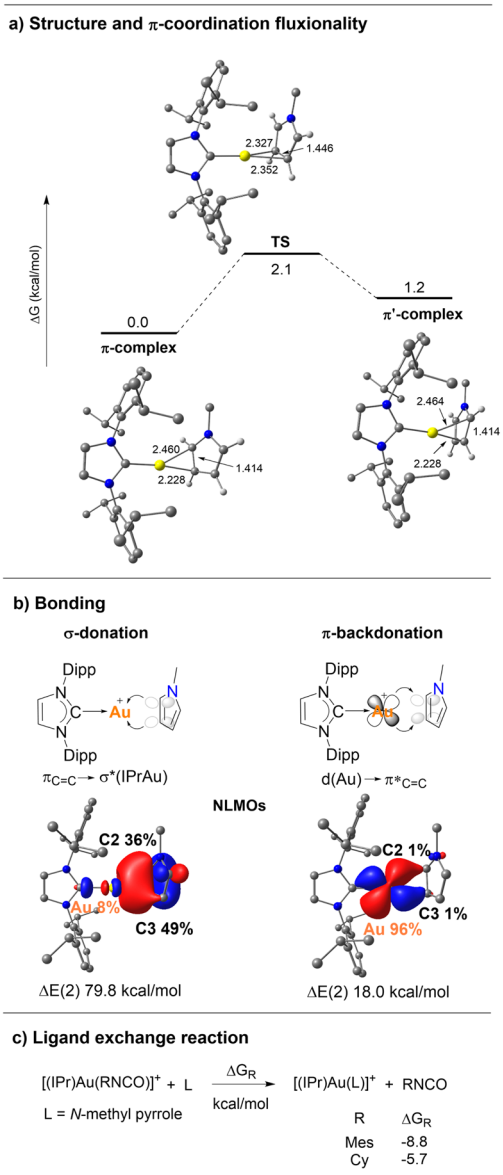

Fig. 7 a) Geometrical data (bond lengths in Å) for the Au(I) *N*-methyl pyrrole π-complex. Optimizations carried out at the SMD(DCM)-PBE0-D3(BJ)/SDD+f(Au), 6-31G** (other atoms) level of theory. Energy profile accounting for its π-coordination fluxionality (ΔG in kcal mol^{-1}). b) Bonding situation from NBO analysis. Plots of the natural localized molecular orbitals (NLMOs) (cutoff: 0.03 a.u.) and the contribution of each atom in percent (%) associated with π(C2═C3) → Au donation and Au → π*(C2═C3) back-donation. Second-order perturbation stabilizing energies $\Delta E(2)$ in kcal mol^{-1}. c) Gibbs free energy (ΔG_R in kcal mol^{-1}) for the ligand exchange between the *N*-adduct of the isocyanate complexes [(IPr)Au(RNCO)]$^+$ (R = Mes, Cy) and *N*-methyl pyrrole.

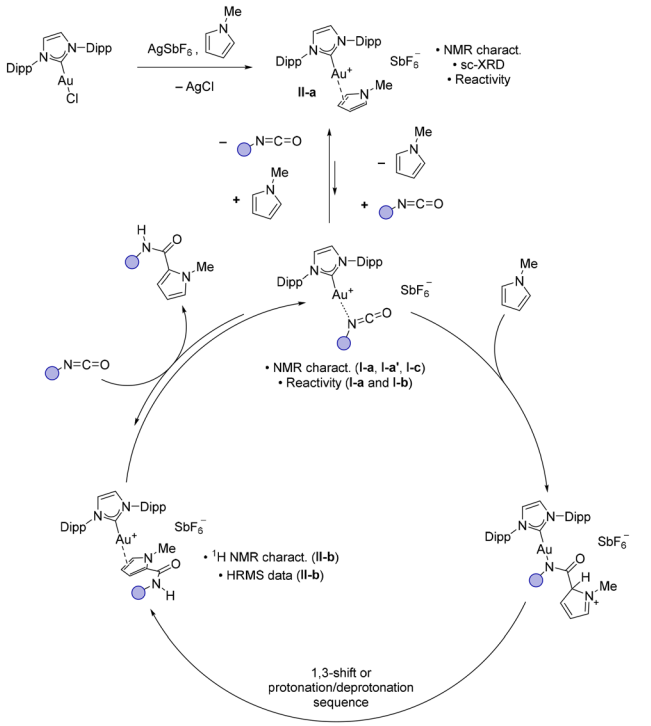

Fig. 8 Catalytic cycle proposed to account for the direct C–H amidation of pyrroles and indoles with isocyanates.

Conclusions

In summary, the first gold-catalyzed hydroarylation of isocyanates was disclosed. While related TM-catalyzed transformations involve insertion of the isocyanate into M–C bonds,[50,51] the Au-catalyzed reaction is proposed to proceed *via* an outer-sphere Friedel–Crafts-type mechanism involving electrophilic activation of the NCO moiety upon *N*-coordination to Au(I) (Fig. 8). Following nucleophilic addition of the pyrrole, either 1,3-H shift or a two-step deprotonation/protonation sequence may occur.

The transformation displays wide generality with respect to the isocyanate, with only a few limitations, namely the *ortho*-disubstituted aryl isocyanates **2m**, the thio-derivative **2u**, and the simple ethyl isocyanate **2t**. Different nucleophiles were successfully employed, tolerating steric hindrance near the reactive carbon atom (**1c** and **1d**) as well as the presence of EWGs on the ring (**1f**). *N*-unprotected indoles, represent the main challenge, due to competitive amidation at the nitrogen atom leading to the corresponding ureas.

Detailed mechanistic studies pointed out the role and structure of Au(I) isocyanate complexes as key reactive intermediates. Several such species have been authenticated by multinuclear NMR spectroscopy at low temperature. The MesNCO complex **I-a**, its ^{15}N-labeled variation **I-a′** and the CyNCO complex **I-c** were thoroughly analyzed, both experimentally and computationally. The end-on *N*-coordination isomer strongly supports the experimental evidence, based on the ^{13}C NMR chemical shift of the NCO signal and the $^{1}J_{CN}$ coupling constant in particular. Additionally, the Au(I) *N*-methyl pyrrole π-complex **II-a** was isolated, fully characterized (NMR and sc-XRD) and authenticated as an off-cycle resting state of the catalytic cycle. Interestingly, complex **II-a** displays dissymmetric η^2-coordination, as reported recently by Guinchard and co-workers for related indole complexes,[45] but in addition, it shows fluxionality as the result of the facile shift of the Au(I) fragment

over the π-system of pyrrole. These results point out the relevance and interest of gold complexes as Lewis acids in the direct C–H amidation of *N*-heterocycles with isocyanates. Extension to other TM and main group (MG)-based Lewis acids and other heteroarenes is certainly worth exploring to further develop the synthetic value of this transformation.

Methods

General procedure for catalytic tests

Inside a glovebox, the gold catalyst (2.5 μmol, 0.5 mol%) and a stoichiometric amount of $AgSbF_6$ or $AgNTf_2$ (2.5 μmol, 0.5 mol%) were placed in a 10 mL Schlenk flask. The flask was then moved into a fume hood, where dimethyl sulfone (internal standard, 10 mg, 0.1 mmol), the solvent (0.75 mL) and *N*-methyl pyrrole (44 μL, 0.5 mmol, 1.0 eq.) were sequentially added under a positive back-flow of argon. The solution was stirred for two minutes, after which a t_0 NMR check was taken. Phenyl isocyanate (54 μL, 0.5 mmol, 1.0 eq.) and $HBF_4{\cdot}Et_2O$ (7.0 μL, 0.05 mmol, 0.1 eq.) were added to the solution, and the reaction mixture was placed in a thermostatic bath at 40 °C. The reaction was monitored over time by ^1H NMR spectroscopy of aliquots sampled from the reaction mixture.

Author contributions

The manuscript was written through contributions of all authors. All authors have given approval to the final version of the manuscript.

Conflicts of interest

There are no conflicts to declare.

Data availability

All experimental, analytical and computational data and NMR and IR spectra are available in the supplementary information (SI) of this article.

Supplementary information is available. See DOI: https://doi.org/10.1039/d6cy00297h.

CCDC 2498446 contains the supplementary crystallographic data for this paper.[52]

Acknowledgements

Financial support from the Centre National de la Recherche Scientifique, the Université de Toulouse and the Agence Nationale de la Recherche (ANR-23-CE07-0008) is gratefully acknowledged. The "Direction du Numérique" of the Université de Pau et des Pays de l'Adour and the Mésocentre de Calcul Intensif Aquitain (MCIA) are acknowledged for their support through computational facilities. This work was also granted access to the HPC resources of IDRIS under the allocation 2024-[AD010800045R3] made by GENCI. F. R. thanks the Ing. Aldo Gini Foundation for the award of a scholarship.

Notes and references

1 D. J. Gorin and F. D. Toste, Relativistic effects in homogeneous gold catalysis, *Nature*, 2007, **446**, 395–403.
2 A. Fürstner and P. W. Davies, Catalytic Carbophilic Activation: Catalysis by Platinum and Gold π Acids, *Angew. Chem., Int. Ed.*, 2007, **46**, 3410–3449.
3 A. Fürstner, From Understanding to Prediction: Gold- and Platinum-Based π-Acid Catalysis for Target Oriented Synthesis, *Acc. Chem. Res.*, 2014, **47**, 925–938.
4 J. H. Teles, S. Brode and M. Chabanas, Cationic Gold(I) Complexes: Highly Efficient Catalysts for the Addition of Alcohols to Alkynes, *Angew. Chem., Int. Ed.*, 1998, **37**, 1415–1418.
5 A. Stephen and K. Hashmi, Homogeneous catalysis by gold, *Gold Bull.*, 2004, **37**, 51–65.
6 A. S. K. Hashmi, Gold-Catalyzed Organic Reactions, *Chem. Rev.*, 2007, **107**, 3180–3211.
7 M. Bandini, Gold-catalyzed decorations of arenes and heteroarenes with C–C multiple bonds, *Chem. Soc. Rev.*, 2011, **40**, 1358–1367.
8 N. Krause and C. Winter, Gold-Catalyzed Nucleophilic Cyclization of Functionalized Allenes: A Powerful Access to Carbo- and Heterocycles, *Chem. Rev.*, 2011, **111**, 1994–2009.
9 M. Rudolph and A. S. K. Hashmi, Gold catalysis in total synthesis—an update, *Chem. Soc. Rev.*, 2012, **41**, 2448–2462.
10 R. Dorel and A. M. Echavarren, Gold(I)-Catalyzed Activation of Alkynes for the Construction of Molecular Complexity, *Chem. Rev.*, 2015, **115**, 9028–9072.
11 A. Quintavalla and M. Bandini, Gold-Catalyzed Allylation Reactions, *ChemCatChem*, 2016, **8**, 1437–1453.
12 D. Campeau, D. F. León Rayo, A. Mansour, K. Muratov and F. Gagosz, Gold-Catalyzed Reactions of Specially Activated Alkynes, Allenes, and Alkenes, *Chem. Rev.*, 2021, **121**, 8756–8867.
13 T. Ghosh, J. Chatterjee and S. Bhakta, Gold-catalyzed hydroarylation reactions: a comprehensive overview, *Org. Biomol. Chem.*, 2022, **20**, 7151–7187.
14 N. Nishina and Y. Yamamoto, Gold-catalyzed hydrofunctionalization of allenes with nitrogen and oxygen nucleophiles and its mechanistic insight, *Tetrahedron*, 2009, **65**, 1799–1808.
15 C. H. Leung, M. Baron and A. Biffis, Gold-Catalyzed Intermolecular Alkyne Hydrofunctionalizations—Mechanistic Insights, *Catalysts*, 2020, **10**, 1210.
16 M. S. M. Holmsen, C. Blons, A. Amgoune, M. Regnacq, D. Lesage, E. D. Sosa Carrizo, P. Lavedan, Y. Gimbert, K. Miqueu and D. Bourissou, Mechanism of Alkyne Hydroarylation Catalyzed by (P,C)-Cyclometalated Au(III) Complexes, *J. Am. Chem. Soc.*, 2022, **144**, 22722–22733.
17 T. Mehrabi and A. Ariafard, The different roles of a cationic gold(I) complex in catalysing hydroarylation of alkynes and alkenes with a heterocycle, *Chem. Commun.*, 2016, **52**, 9422–9425.

18 A. Zhdanko and M. E. Maier, The Mechanism of Gold(I)-Catalyzed Hydroalkoxylation of Alkynes: An Extensive Experimental Study, *Chem. – Eur. J.*, 2014, **20**, 1918–1930.
19 N. D. Shapiro and F. D. Toste, Synthesis and structural characterization of isolable phosphine coinage metal π-complexes, *Proc. Natl. Acad. Sci. U. S. A.*, 2008, **105**, 2779–2782.
20 H. Schmidbaur and A. Schier, Gold η^2 -Coordination to Unsaturated and Aromatic Hydrocarbons: The Key Step in Gold-Catalyzed Organic Transformations, *Organometallics*, 2010, **29**, 2–23.
21 H. V. R. Dias, J. A. Flores, J. Wu and P. Kroll, Monomeric Copper(I), Silver(I), and Gold(I) Alkyne Complexes and the Coinage Metal Family Group Trends, *J. Am. Chem. Soc.*, 2009, **131**, 11249–11255.
22 M. A. Celik, C. Dash, V. A. K. Adiraju, A. Das, M. Yousufuddin, G. Frenking and H. V. R. Dias, End-On and Side-On π-Acid Ligand Adducts of Gold(I): Carbonyl, Cyanide, Isocyanide, and Cyclooctyne Gold(I) Complexes Supported by N-Heterocyclic Carbenes and Phosphines, *Inorg. Chem.*, 2013, **52**, 729–742.
23 M. Navarro, A. Toledo, S. Mallet-Ladeira, E. D. Sosa Carrizo, K. Miqueu and D. Bourissou, Versatility and adaptative behaviour of the P^N chelating ligand MeDalphos within gold(I) π complexes, *Chem. Sci.*, 2020, **11**, 2750–2758.
24 M. Navarro and D. Bourissou, in *Adv. Organomet. Chem.*, ed. P. J. Pérez, Academic Press, 2021, pp. 101–144.
25 J. Mehara, B. T. Watson, A. Noonikara-Poyil, A. O. Zacharias, J. Roithová and H. V. Rasika Dias, Binding Interactions in Copper, Silver and Gold π-Complexes, *Chem. – Eur. J.*, 2022, **28**, e202103984.
26 C. L. Johnson, D. J. Storm, M. A. Sajjad, M. R. Gyton, S. B. Duckett, S. A. Macgregor, A. S. Weller, M. Navarro and J. Campos, A Gold(I)–Acetylene Complex Synthesised using Single-Crystal Reactivity, *Angew. Chem., Int. Ed.*, 2024, **63**, e202404264.
27 R. S. Ramón, S. Gaillard, A. Poater, L. Cavallo, A. M. Z. Slawin and S. P. Nolan, [{Au(IPr)}$_2$(μ-OH)]X Complexes: Synthetic, Structural and Catalytic Studies, *Chem. – Eur. J.*, 2011, **17**, 1238–1246.
28 I. Shehadi, F. Abla, B. Wakefield, J. Reibenspies, M. Arooj and A. A. Mohamed, Facile protic hydration of acetonitrile to protonated acetamide at oxygen mediated by chloroauric acid: insights from experimental and calculations, *Res. Chem. Intermed.*, 2020, **46**, 593–607.
29 J. Wu and Z. Xia, Gold-Catalyzed Redox-Neutral Reaction of Nitriles with Quinoline N-Oxides, *Adv. Synth. Catal.*, 2023, **365**, 3335–3341.
30 Y. Wu, B. Tian, S. Witzel, H. Jin, X. Tian, M. Rudolph, F. Rominger and A. S. K. Hashmi, $AuBr_3$-Catalyzed Chemoselective Annulation of Isocyanates with 2H-Azirine, *Chem. – Eur. J.*, 2019, **25**, 4093–4099.
31 P. Braunstein and D. Nobel, Transition-metal-mediated reactions of organic isocyanates, *Chem. Rev.*, 1989, **89**, 1927–1945.
32 See Supporting Information for details.
33 M. Baron and A. Biffis, Gold(I) Complexes in Ionic Liquids: An Efficient Catalytic System for the C-H Functionalization of Arenes and Heteroarenes under Mild Conditions, *Eur. J. Org. Chem.*, 2019, **2019**, 3687–3693.
34 S. Bonfante, P. Bax, M. Baron and A. Biffis, Gold(I)-Catalyzed Direct Alkyne Hydroarylation in Ionic Liquids: Mechanistic Insights, *Catalysts*, 2023, **13**, 822.
35 P. Bax, F. Ravera, S. Bonfante, F. Floreani and A. Biffis, Direct Coumarin Synthesis by Gold Catalyzed Hydroarylation of Alkynoic Acids/Esters, *ChemCatChem*, 2025, **17**, e00465.
36 F. Ravera, F. Floreani, C. Tubaro, M. Roverso, R. Pedrazzani, M. Bandini and A. Biffis, An Improved Gold(I) Catalytic System for the Preparation of Coumarins via Intramolecular Cyclization, *Chem. – Asian J.*, 2025, **20**, e202400725.
37 A. Dasgupta, Y. van Ingen, M. G. Guerzoni, K. Farshadfar, J. M. Rawson, E. Richards, A. Ariafard and R. L. Melen, Lewis Acid Assisted Brønsted Acid Catalysed Decarbonylation of Isocyanates: A Combined DFT and Experimental Study, *Chem. – Eur. J.*, 2022, **28**, e202201422.
38 M. Jia and M. Bandini, Counterion Effects in Homogeneous Gold Catalysis, *ACS Catal.*, 2015, **5**, 1638–1652.
39 Z. Lu, J. Han, O. E. Okoromoba, N. Shimizu, H. Amii, C. F. Tormena, G. B. Hammond and B. Xu, Predicting Counterion Effects Using a Gold Affinity Index and a Hydrogen Bonding Basicity Index, *Org. Lett.*, 2017, **19**, 5848–5851.
40 J. Schießl, J. Schulmeister, A. Doppiu, E. Wörner, M. Rudolph, R. Karch and A. S. K. Hashmi, An Industrial Perspective on Counter Anions in Gold Catalysis: Underestimated with Respect to 'Ligand Effects', *Adv. Synth. Catal.*, 2018, **360**, 2493–2502.
41 D. Wang, R. Cai, S. Sharma, J. Jirak, S. K. Thummanapelli, N. G. Akhmedov, H. Zhang, X. Liu, J. L. Petersen and X. Shi, 'Silver Effect' in Gold(I) Catalysis: An Overlooked Important Factor, *J. Am. Chem. Soc.*, 2012, **134**, 9012–9019.
42 P. La Manna, C. Talotta, M. De Rosa, A. Soriente, C. Gaeta and P. Neri, An Atom-Economical Method for the Formation of Amidopyrroles Exploiting the Self-Assembled Resorcinarene Capsule, *Org. Lett.*, 2020, **22**, 2590–2594.
43 L. Chen, C. Li, H. Wang, J. Li and S. Song, HFIP-Promoted Aromatic Electrophilic Amidation of Indoles and Pyrroles with Isocyanates, *J. Org. Chem.*, 2025, **90**, 4271–4276.
44 Z. Li, R. J. Mayer, A. R. Ofial and H. Mayr, From Carbodiimides to Carbon Dioxide: Quantification of the Electrophilic Reactivities of Heteroallenes, *J. Am. Chem. Soc.*, 2020, **142**, 8383–8402.
45 P. Milcendeau, M. Ramdani, E. van Elslande and X. Guinchard, Cationic Au(I) Complexes of Indoles, *ACS Org. Inorg. Au*, 2025, **5**, 485–491.
46 E. Herrero-Gómez, C. Nieto-Oberhuber, S. López, J. Benet-Buchholz and A. M. Echavarren, Cationic η^1/η^2-Gold(I) Complexes of Simple Arenes, *Angew. Chem., Int. Ed.*, 2006, **45**, 5455–5459.
47 V. Lavallo, G. D. Frey, S. Kousar, B. Donnadieu and G. Bertrand, Allene formation by gold catalyzed cross-coupling of masked carbenes and vinylidenes, *Proc. Natl. Acad. Sci. U. S. A.*, 2007, **104**, 13569–13573.

48 M. Navarro, A. Toledo, M. Joost, A. Amgoune, S. Mallet-Ladeira and D. Bourissou, π Complexes of P^P and P^N chelated gold(I), *Chem. Commun.*, 2019, **55**, 7974–7977.
49 M. Navarro, M. Holzapfel and J. Campos, A Cavity-Shaped Gold(I) Fragment Enables CO_2 Insertion into Au–OH and Au–NH Bonds, *Inorg. Chem.*, 2023, **62**, 10582–10591.
50 J. R. Hummel, J. A. Boerth and J. A. Ellman, Transition-Metal-Catalyzed C–H Bond Addition to Carbonyls, Imines, and Related Polarized π Bonds, *Chem. Rev.*, 2017, **117**, 9163–9227.
51 E. Serrano and R. Martin, Forging Amides Through Metal-Catalyzed C–C Coupling with Isocyanates, *Eur. J. Org. Chem.*, 2018, **2018**, 3051–3064.
52 CCDC 2498446: Experimental Crystal Structure Determination, 2026, DOI: 10.5517/ccdc.csd.cc2pvv1g.